Journal of the Korean Ceramic Society
Vol. 45, No. 12, pp. 815~820, 2008.

Characterization of Mechanical Alloying Processed Ti-Si-B Nanocomposite Consolidated by Spark Plasma Sintering

Hyung-Bock Lee†, In-Jong Kwon, Hyung-Jik Lee*, and Young-Hwan Han**

Department of Materials Science & Engineering, Myong-Ji University, Yongin 449-728, Korea
**Department of Materials Science & Engineering, Kang-Nung University, Kangnung 210-702, Korea*
***Department of Chemical Engineering & Materials Science, University of California, Davis CA 95616, USA*
(Received October 13, 2008; Revised November 7, 2008; Accepted November 13, 2008)

ABSTRACT

The microstructure and mechanical properties of TiB_2/Si nanocomposites based on the Ti-Si-B system, consolidated by spark plasma sintering of mechanically alloyed activated nanopowders, have been characterized. Mechanical Alloying was carried out in a planetary ball mill for 180 min with 350 rev min^{-1}. The powders were pressed in vacuum at a pressure of 60 MPa, generating a maximum temperature in the graphite mould of 1400°C. Analysis of the synthesized nanocomposites by SEM, XRD and TEM showed them to consist of TiB_2 second phase, sub-micron in size, with no third phase. Composites consolidated from powders mechanically alloyed from an initial elemental powder mix of 0.3 mol Si, 0.7 mol Ti, and 2.0 mol B achieved the best relative density (97%) and bending strength (774 MPa); the highest Vickers hardness of 14.7 GPa was achieved for the 0.1-0.9-2.0 mol starting composition.

Key Words **: *Spark plasma sintering, Mechanical alloying, Ti-Si-B system, Planetary mill, Activated powder, Nanocomposite***

1. Introduction

TiB_2 in boride ceramics is known more for its diverse character, rather than both metal and ceramic, due to its high melting point, remarkable hardness, chemical stability, and high electrical conductivity, like metal. Thus, TiB_2 is expected for applications with high-temperature materials, high speed cutting tools, surface protection, armor cladding materials, Al smelting, electrodes for MHD generators and anti-abrasives in corrosive environments. Despite its exceptional structural and electrical properties, TiB_2 ceramics are known to be very difficult to consolidate due to strong covalence and thermal expansion anisotropy. The conventional consolidation method heats elements or mixtures up to near their melting points, consuming high energy and reaching almost full densification.[1] Recently, abundant research has been focusing on both adding metal or ceramic to TiB_2 to improve its mechanical property by suppressing grain growth, and also a new technique being developed to solve difficulty in consolidation of TiB_2.[2-4] Mechanical Alloying and Spark Plasma Sintering (SPS) techniques are well attended for this purpose. Mechanical Alloying uses ball milling with high mechanical energy for a new synthetic powder through a self-reacting process, which is very different from the original powder in character and microstructure. SPS is well known for faster time in the consolidation process.

Mechanical Alloying technique is widely used for nano material processing. The principle of the technique is that powders keep pressing and fracturing among the balls to make a homogeneously and finely dispersed alloying solid phase without making a liquid phase around room temperature, expecting superior compositional property to rapid cooling or metal matrix composite phase hardening technique.[5,6] Moreover, SPS makes ceramic powder denser and more rapidly in consolidation by sparking electron plasma among particles. During sparking, the surface of the particles become instantly activated and refined, generating self-heating among particles leading to thermal change and mass change in a very short time. Thus, rapid densification is possible through a micro scale heating process.

When synthetic powders by Mechanical Alloying process are pressed by SPS, it has an advantage due to lower synthesizing temperature with particle surface activation and consumes less time in consolidation, and can help to achieve denser matrix and finer microstructure at the same time.[8-12] The purpose of the study is to show that the Ti-Si-B nanocomposite is consolidated by SPS from Mechanical Alloying processed synthetic composite powders by planetary mill, for characterization from microstructures and measurement of mechanical properties.

†Corresponding author : Hyung-Bock Lee
E-mail : mjhblee@mju.ac.kr
Tel : +82-31-330-6459 Fax : +82-31-330-6457

2. Experimental Procedures

2.1. Mechanical alloying process

Table 1. Experimental Composition of Ti, Si and B Powders

Starting materials	Composition (mol)		
	0.1	0.3	0.5
Titanium	0.9	0.7	0.5
Silicon	0.1	0.3	0.5
Boron	2.0	2.0	2.0

Starting powder elements used were; Ti (Osaka Titanium Co, 99.0% purity, −325 mesh), B (Aldrich Chemical Co, 95.0% purity, −325 mesh), and Si (Junsei Chemical Co, 99.0% purity, −325 mesh). Experimental compositions are shown in Table 1 with the Mechanical Alloying processed for the compositions. Mechanical Alloying was performed in a planetary ball mill with a ball/powder ratio of 10:1 at 350 rev min^{-1}. Milling in a vacuum was continued until no further reaction was observed for 180~210 min. Samples were checked by XRD every 30 min to determine the progress of synthesis.

2.2. Consolidation processing of the nanocomposite

The powder obtained just before synthesis by Mechanical Alloying was complete was chosen for consolidation to minimize grain growth and allow full densification at low synthesis temperature. As shown in the overview of SPS in Fig. 1, the mixture was loaded and pressed under 60 MPa in a vacuum (10^{-3} torr), with 1800 A dc electrical current was applied until a temperature of 1400°C was reached on the surface of a graphite mold with 12/2 in on/off time. It took about 4 min to reach at 1400°C, after which the power was switched off, allowing the chamber to cool down. Fig. 2 is a schematic diagram of the process.

2.3. Microstructural analysis and measuring mechanical properties

Synthesized powders and the phases in the sintered body were analyzed by XRD (Shimadzu Co. model XD-DI, Cu kα). Microstructure and particle size in the compositions were observed by SEM (Phillips Co. 515) and TEM (Joel Co. JEM-3011), and quantitative phase analysis was conducted using EDS (Leica Cambridge Ltd, Oxford). The density of sintered body was determined according to Korean Standard KSL 3114 for porosity, absorption, and specific gravity measurement method in refractory bricks. The sintered specimen was boiled at 100°C for 3 hours to calculate the volume from the weight of buoyancy and bubbles for dry weight. To obtain the relative density of the composite, specific weight was divided by theoretical density.

An Instron mechanical tester (Instron Japan, model 4204) was used at 0.5 mm min^{-1} cross-head speed, with 15 mm span distance for three point bending strength applying a fracture load. For hardness measurement, a Vickers hardness indenter was applied to the polished surfaces under a load of 10 kgf for 10 s at 50 μm s^{-1}.

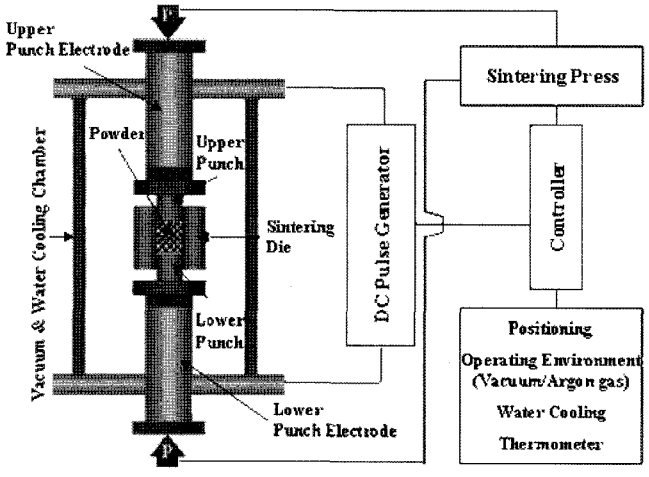

Fig. 1. Overview and schematic diagram of SPS process.

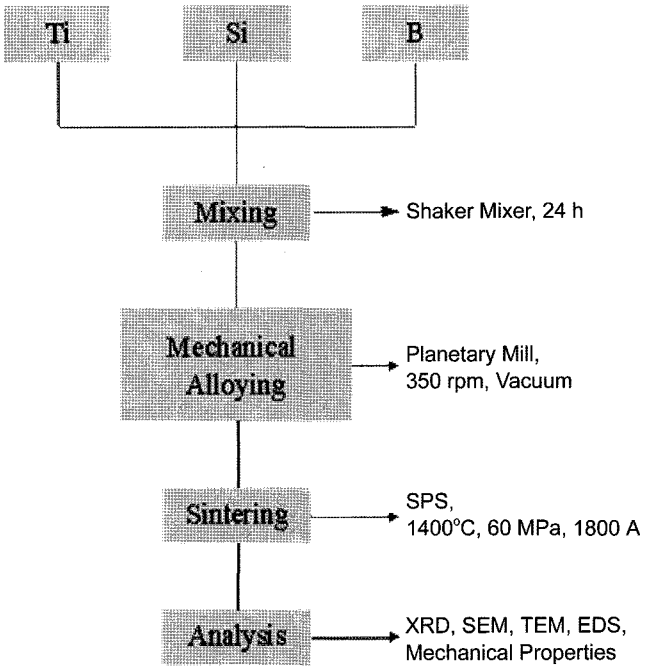

Fig. 2. Flow chart of experimental procedure.

3. Discussion and Results

3.1. Characteristics of synthesized powder

Ordinary ball milling requires a very long milling time due to lack of collision energy for mechanical alloying effect. Planetary ball milling technique allows for changing the jar's direction and rotation for the high energy required in milling. Phase transformations occurring in the powders on ratio of balls and several compositions during milling were observed with time.

XRD scans for three initial powder mixes with time as mechanical alloying processes were shown in Figs. 3~5. The peaks of the initial powders tend to become weaker but broader with time, a common tendency in mechanical alloying that results from the internal stress and high densities of lattice defects in the powder and leads to microstructural

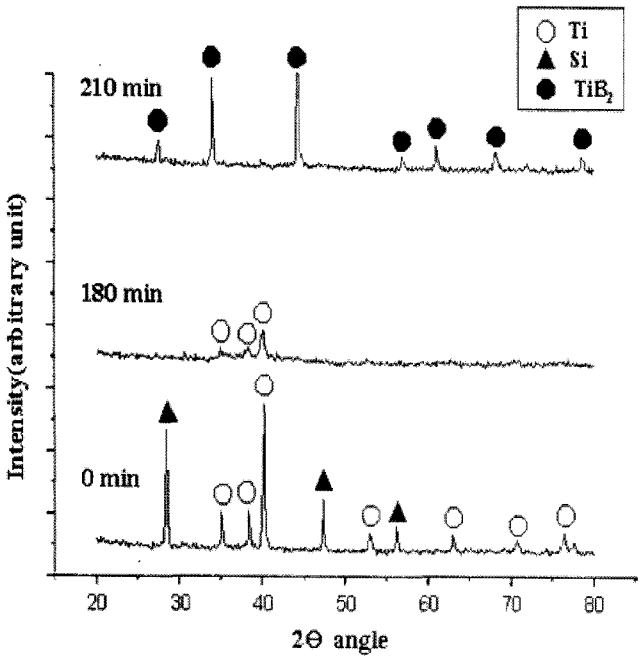

Fig. 3. X-ray diffraction patterns of the mechanical alloyed composition 0.3 as function of milling time.

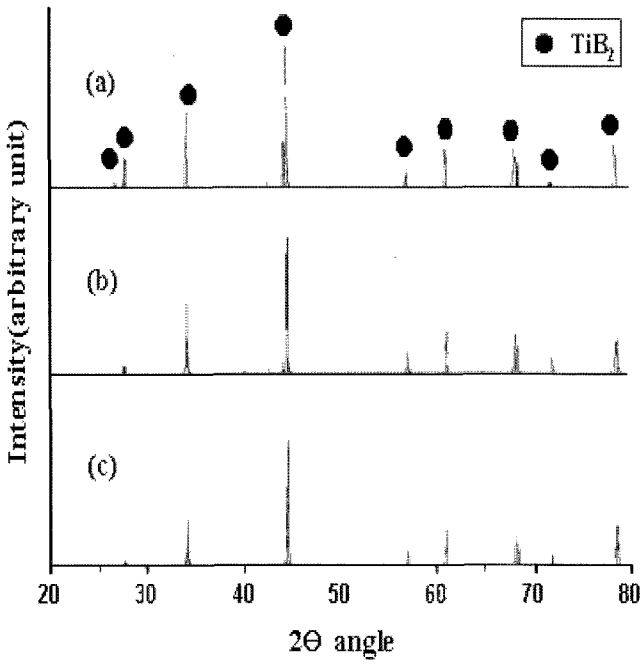

Fig. 4. X-ray diffraction patterns of Ti-Si-B composites sintered by SPS; (a) 0.1, (b) 0.3, and (c) 0.5.

refinement by contact press, fracture, and powder homogenization and in some instances, to impact energy of the ball mill.[7]

Increasing milling time up to 180~210 min generated a sudden change of phase, with the appearance of new peaks representing TiB_2 and the disappearance of Ti and Si peaks. At room temperature, synthesis appears to occur by SHS (self-propagating high temperature synthesis) during the milling process with no induction of direct or indirect thermal energy.[9-12] Generating more homogenized and contact surface area by grinding the powder mixture to a smaller size, just before the complete synthesis stage, during mechanical alloying would be beneficial with higher activation, leading to a lower synthesis temperature.[13]

3.2. Characteristics of the sintered body

The XRD pattern of the sintered body consolidated by SPS shows TiB_2 peaks only, as shown in Fig. 4. No Si peaks are detected, although the higher Si compositions have lower TiB_2 peak intensity. Residual Si on TiB_2 grain boundaries seems to remain in an amorphous state during rapid cooling after the synthesis process of TiB_2 by SPS.

Fracture surfaces of Ti-Si-B composites by SPS are shown in Fig. 5. In general, with increasing Si content, the presence of a greater quantity of liquid phase would be expected to separate the boride particles, resulting in a more typical morphology of interfacial fracture.

Many similar phenomena have been observed in the present Ti-Si-B system with the results of the Ti-Al-B system, published by Lee et al.[15]

Fig. 5(a) (0.1 mol Si) shows the largest particle size, 1.0~1.5 μm, but seems denser, maintaining irregular distribution of Si over the fracture surface. Fig. 5(b) (0.3 mol Si), with smaller particle size, indicating the smallest particle of Si on the fracture surface that could act as a fracture initiating defect. In Fig. 5(c) (0.5 mol Si), precipitated excessive Si

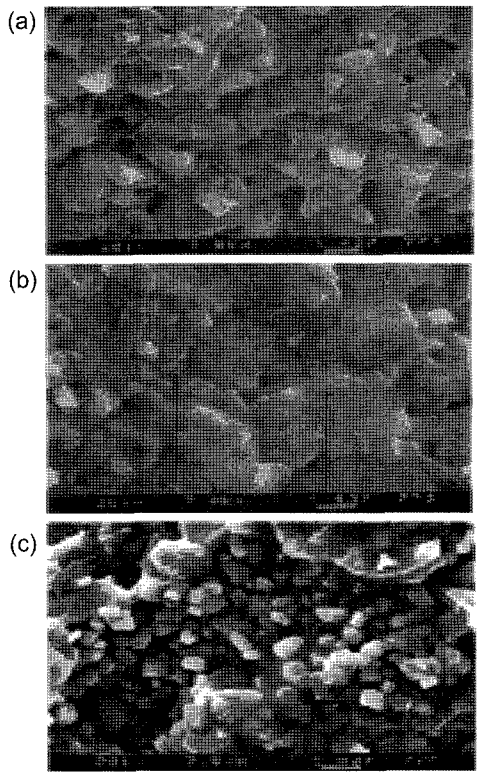

Fig. 5. SEM photographs of Ti-Si-B composite sintered by SPS; (a) 0.1, (b) 0.3, and (c) 0.5.

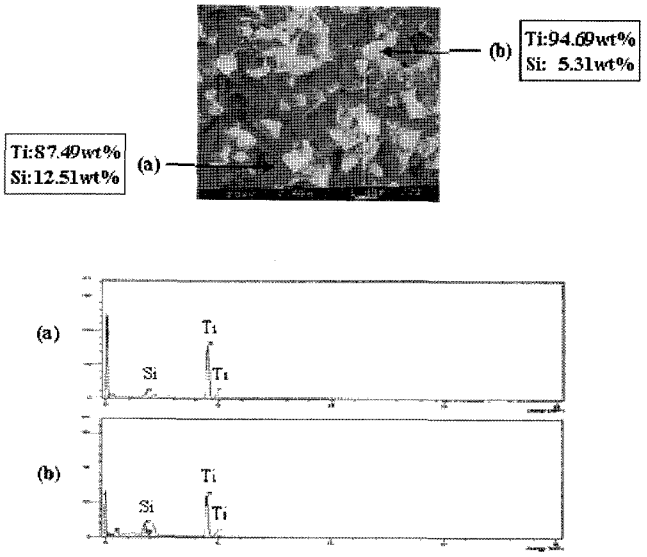

Fig. 6. EDS result of composition 0.1 sintered by SPS.

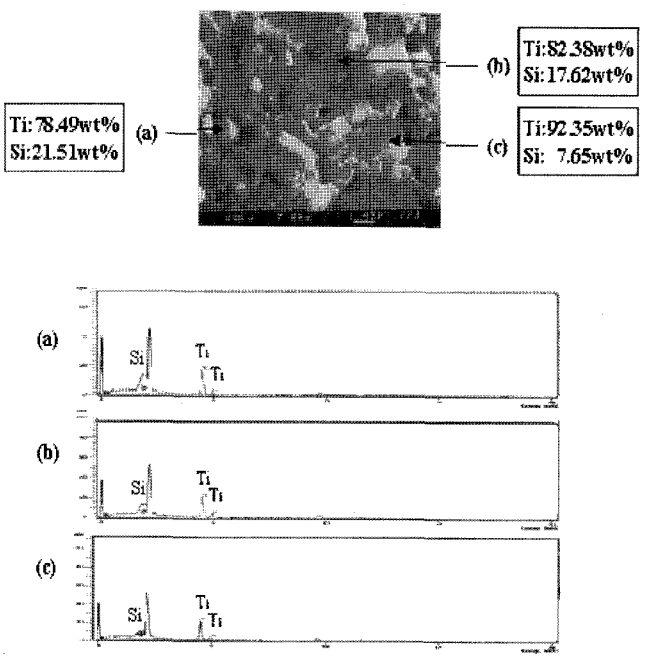

Fig. 7. EDS result of composition 0.3 sintered by SPS.

exists on the segregated TiB_2 particle faces, presumably as a result of the presence of a liquid phase, leading to more porosities causing less densification, during the rapid cooling process following SPS.[14]

EDS was performed for compositional analysis on interesting microstructures detected in the SEM micrographs, as shown in Figs. 6~8.

In Fig. 6(a) (0.1 mol Si), 87.5 wt% Ti, 12.5 wt% Si detected, and in Fig. 7(b) (0.3 mol Si), 94.7 wt% Ti, 5.3 wt% Si with undetectable B in EDS, but assumed as TiB_2 particle by XRD. In Fig. 8 (0.5 mol Si), fine particle at (a) is considered to be TiB_2 phase. In Fig. 7(b) and (c) (0.3 mol Si), 82.4 wt% Ti, 17.6 wt% Si detected and 92.4 wt% Ti, 7.6 wt%

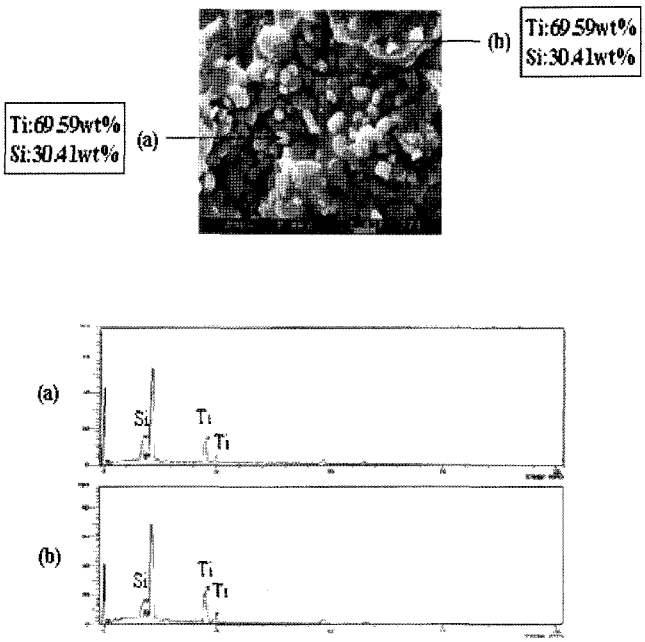

Fig. 8. EDS result of composition 0.5 sintered by SPS.

Si. It is close to the composition of the 0.1 mol Si and, in Fig. 7(a) (0.3 mol Si), 78.5 wt% Ti, 21.5 wt% Si, some increase in Si ratio than (b), (c). It seems that Si is inhomogeneously distributed and, therefore, varies in weight percentage. In Fig. 8 (0.5 mole Si), 69.6 wt% Ti and 30.4 wt% Si were detected in the same amount in (a) and (b).

While XRD of the sintered body did not reveal the presence of Si, EDS analyzed considerable content of Si from the body, suggesting that Si and/or Ti silicide exist in an amorphous state as a ternary phase on the TiB_2 grain boundaries. The microfine and highly activated powders just before synthesis used in the present research, which was

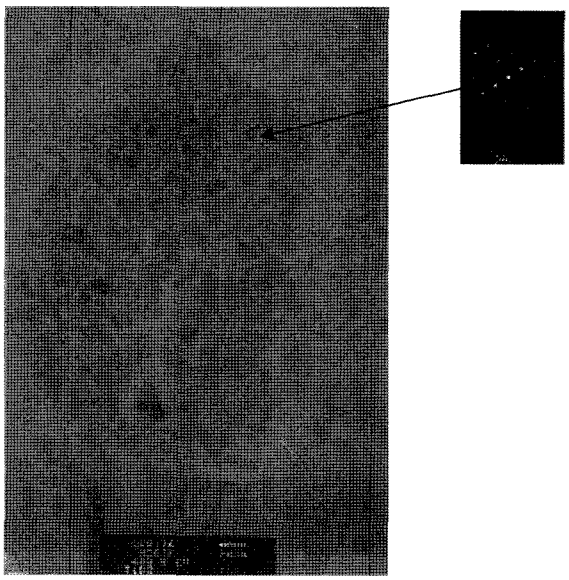

Fig. 9. TEM micrographs of Ti-Si-B composite sintered by SPS.

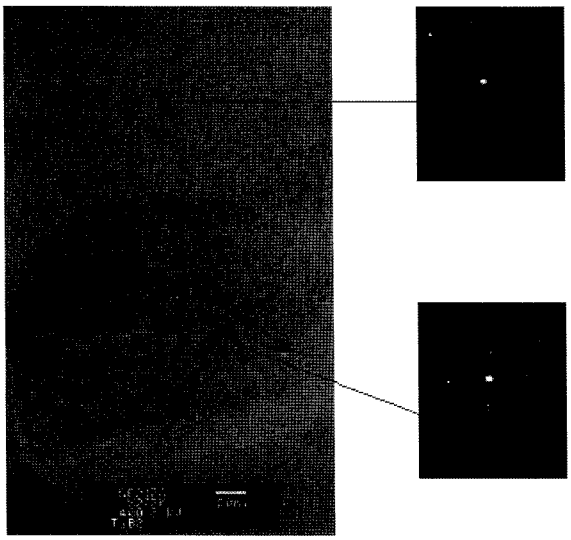

Fig. 10. TEM micrographs of Ti-Si-B composite sintered by SPS.

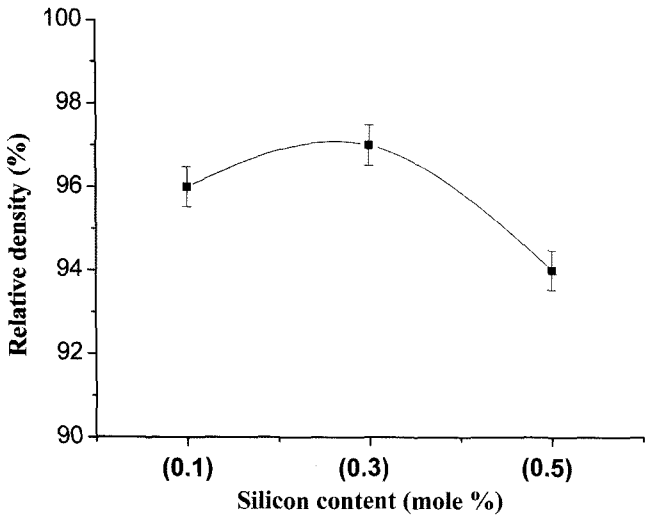

Fig. 11. Relative density of Ti-Si-B composites sintered by SPS.

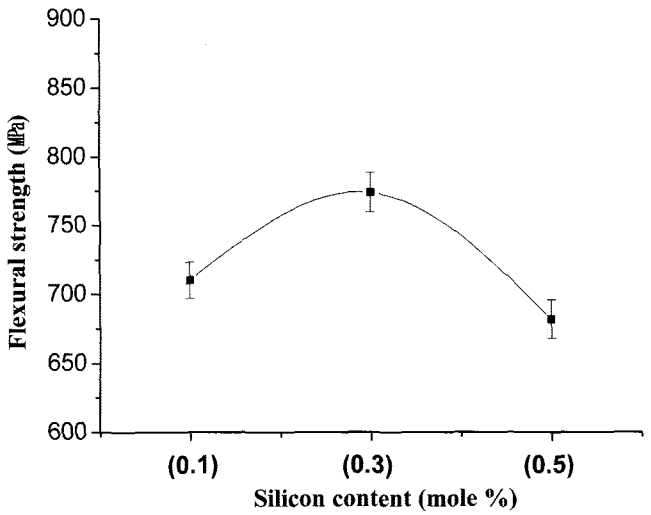

Fig. 12. Flexural strength of Ti-Si-B composites sintered by SPS.

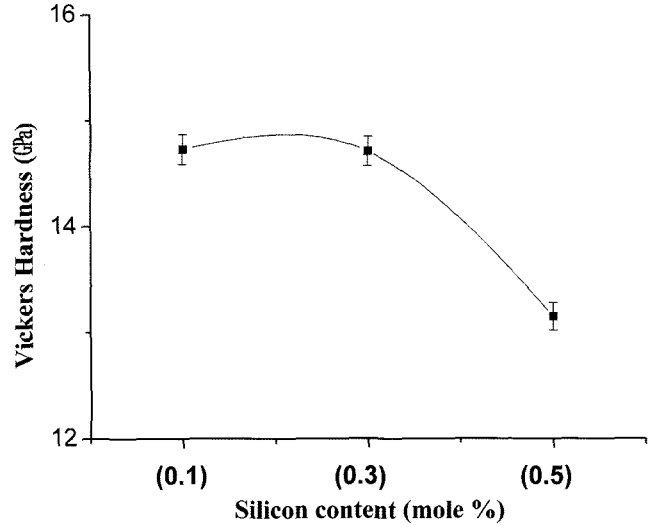

Fig. 13. Vickers hardness of Ti-Si-B composites sintered by SPS.

processed by mechanical alloying and SPS with low sintering temperature and time, appear to have suppressed grain growth. Thus, the large particles observed appear to be nanosize TiB_2 with an amorphous Si, Ti silicide third phase(s) present at grain boundaries.

Transmission electron microscopy was performed on a film specimen from the bulk body, which was machined and ion milled by a Gatan PIPS ion miller.

Fig. 9 shows a TEM micrograph of a Ti-Si-B composite of about 300 nm particle size, in which numerous grain boundaries surrounding particles exist.

Fig. 10 shows particles on part (a) consist of mostly Ti, to be considered TiB_2 crystalline structure.

The crystalline structure tending to be spherical, which was pressed and plasma sintered, prohibits grain growth in a short sintering time. The dark part (b) consists of Si, which mixed with unreacted Ti and B, as a ternary amorphous phase.

Fig. 11 shows the relative density of Ti-Si-B nanocomposite consolidated by SPS. As noted in the SEM micrograph, the 0.3 mole Si composition considered the densest has a higher value of 97% than 0.1 mol Si in 96%, and in the 0.5 mole Si composition with low relative density of 94%, liquid phase formation is getting more active with increasing Si addition, inducing cracking inside phases during rapid cooling with a short sintering time. Addition of Si enhances densification to some extent, but overdose of Si prevents densification with internal cracking.

Fig. 12 shows the bending strength of the compositions of Si in the composite.

All three compositions have very high strength values of 682~774 MPa, the highest (774 MPa) being the 0.3 mol Si composition. This excellent strength in the Ti-Si-B system can be explained in terms of both full densification by liquid

phase sintering with Si addition and prevention of grain growth staying at the nanosize level and also increasing relative crack length in fracturing. The 0.5 mol Si composition has the lowest value (682 MPa), and it is considered to be overdosed after 0.3 mol Si, leading to aggravation in strength improvement.

Fig. 13 shows Vickers hardness measurements for the Ti-Si-B composites. Hardness decreased with higher Si content, presenting higher 14.73 GPa and 14.71 GPa in the 0.1 and the 0.3 mol Si compositions and the lowest value of 13.2 GPa in the 0.5 mol Si composition.

4. Conclusions

The activated nanopowders by mechanical alloying were processed, and then pressed by SPS at 1400°C under 60 MPa for Ti-Si-B nanocomposite as below,

1) Ti-Si-B system was very similar in the aspects of Ti-Al-B system.
2) The TiB_2 was synthesized by mechanical alloying process, proved by XRD and SEM.
3) Ti-Si-B nanocomposite was successfully consolidated by SPS, and sub-micron TiB_2 crystalline particles were observed by SEM.
4) Composite of the 0.3 mol Si, 0.7 mol Ti, and 2.0 mol B achieved the best relative density (97%) and bending strength (774 MPa), and the highest Vickers hardness of 14.7 GPa was achieved for the 0.1-0.9-2.0 mol starting composition.

Acknowledgment

The authors are pleased to acknowledge many useful discussions with special thanks to Dr. Ellen Heian at UC Davis for the interpretation of TEM micrographs.

REFERENCES

1. E. S. Kang, D. I. Chungand, and Y. K. Paek, "The Effects of Sintering Aids on The Sintering Behavier of TiB_2-Based Ceramics," *Ceramic Armor Material Conference,* 25-44 (1990).
2. J. A. Kuszyk and R. C. Bradt, "Influence of Grain Size on Effects of Thermal Expansion Anisotropy in $MgTi_2O_5$," *J. Am. Ceram. Soc.,* **56** [8] 420-23 (1973).
3. C. F. Yen, C. S. Yust, and G. W. Clark, "Enhancement of Mechanical Strength in Hot-Pressed TiB_2 Composites by The Addition of Fe and Ni," pp. 317-30 in New Developments and Applications in Composites, Trans., AIME, Warrendal, Penn., 1979.
4. R. Z. Yuan, Z. Y. Fu, Z. A. Munir, X. X. Zhou, and Z. L. Yang, "Fabrication of Dense TiB_2-Al Composites by The Self-Propagating High-Temperature Synthesis(SHS) Method," *J. Mater. Synth. Proc.,* **1** [3] 153-57 (1993).
5. G-G Lee., "Development and Application of Mechanical Alloying," *J. Kor. Powder Metall. Ins.,* **9** [1] 61-5 (2002).
6. Z. Xinkun, Z. Kunyu, C. Baochang, L. Qiushi, and Z. Xiuqin, "Synthesis of Nanocrystalline TiC Powder by Mechanical," Materials Science & Engineering, C, Biomimetic and Supramolecular Systems, **16** 103-5 (2001).
7. F. H. Froes, K. Russell, C. -G. Lic, F.H. S. Froes, and C. Suryanarayana, "Synthesis of Intermetallics by Mechanical alloying," *Mater. Sci. Eng. A,* **192-193** [2] 612-23 (1995).
8. N.F. Gaoa, J.T. Lib, D. Zhangc, and Y. Miyamotoa, "Rapid Synthesis of Dense Ti_3SiC_2 by Spark Plasma Sintering," *J. Eur. Ceram. Soc.,* **22** 2365-70 (2002).
9. M. Tokita, "The Mechanism of Spark Plasma Sinering," *Proc. 2th Symp. On SPS,* 1-7 (1997).
10. M. Tokita, "Development of Large-size Ceramic/Metal Bulk FGM Fabricated by Spark Plasma Sintering," *Proc. 5th int. Symp. on FGM,* 83-8 (1998).
11. N. Tamari, T. Tanaka, K. Tanaka, and M. Tokita, "Effect of Spark Plasma Sintering on Densification and Mechanical Properties of Silicon Carbide," *J. Ceram. Soc. Jpn.,* **103** [7] 740-42 (1995).
12. M. Tokita, "Trends in Advanced Spark Plasma Sintering Systems and Technology," *J. Soc. Powder Tech, Jpn.,* **30** [11] 790-804 (1993).
13. M. A. Venkataswamy, J. A. Schneider, J. R. Groza, A. K. Mukherjee, K. Yamazaki, and K. Shoda, "Mechanical Alloying Processing and Rapid Plasma Activated Sintering Consolidation of Nanocrystalline Iron-Aluminides," *J. Mater. Scie. Eng. A,* **207** 153-58 (1996).
14. J.-K. Lee, H.-H. Kim, J.-G. Park, and E.-G. Lee, "Influence of Liquid-Phase Amount on the Microstructure and Phase Transformation of Liquid-phase Sintered Silicon Carbide," *J. Kor. Ceram. Soc.,* **35** [4] 413-19 (1998).
15. H.B. Lee, S.H. Kim, S.W. Kang, and Y.H. Han, "Characterisation of Mechanically Alloyed Ti-Al-B Nanocomposite Consolidated by Spark Plasma Sintering," *British Ceramic Transactions.,* **102** [6] 231-36 (2003).